Chapter 6

Flows

6.1 Definition of Dynamical Systems

Definition: A dynamical system is a set of ordinary differential equations of the form

$$\frac{dx_i}{dt} = F_i(x; c) \tag{6.1}$$

Here $x = (x_1, x_2, \cdots, x_n) \in R^n$ are called *state variables* and $(c_1, c_2, \cdots, c_k) \in R^k$ are called *control parameters*. The functions $F_i(x; c)$ are assumed to be 'sufficiently smoothe.'

Remark: The state variables and control parameters are usually considered to be in subspaces of euclidean spaces, but they may more generally be in n- and k-dimensional manifolds.

Remark: The space of state variables is often called the *phase space*.

Remark: Initial conditions for any solution of the dynamical system equations belong in the phase space.

Remark: The functions $F_i(x; c)$ are usually assumed to be differentiable over the region of interest, but a Lipschitz condition $|F(x; c) - F(x'; c)| < K(c)|x - x'|$ is sufficient for the most important properties of dynamical systems which we will exploit: the existence and uniqueness theorem (*c.f.*, Sec. 6.2). In most cases of interest, the functions $F_i(x; c)$ are polynomials in the x_j whose coefficients depend on the control parameters c. Such functions are Lipschitz on bounded domains in R^n.

Remark: If the functions $F_i(x; c)$ are not explicitly dependent on time (*i.e.*, $\partial F_i/\partial t = 0$, all i) the system is said to be *autonomous*. Otherwise, it is said to be *nonautonomous*. It is often possible to replace a nonautonomous system of equations in n dimensions by an autonomous system of equations in higher dimensions. We will see how this can be done in the two examples of periodically driven systems discussed below.

6.2 Existence and Uniqueness Theorem

The fundamental theorem for dynamical systems is the Existence and Uniqueness theorem, which we state here without proof.

Theorem: If the dynamical system (6.1) is Lipschitz in the neighborhood of a point x_0, then there is a positive number s, and

Existence: there is a function $\phi(t) = (\phi_1(t), \phi_2(t), \cdots, \phi_n(t))$ which satisfies the dynamical system equations $d\phi_i(t)/dt = F_i(\phi(t); c)$ in the interval $-s \leq t \leq +s$, with $\phi(0) = x_0$;

Uniqueness: the function $\phi(t)$ is unique.

This is a *local* theorem. It guarantees that there is a unique nontrivial trajectory through each point at which a dynamical system satisfies the Lipschitz property. If the dynamical system is Lipschitz throughout the domain of interest, this local theorem is easily extended to a global theorem.

Global Theorem: If the dynamical system (6.1) is Lipschitz, then there is a unique trajectory through every point, and that trajectory can be extended asymptotically to $t \to \pm\infty$.

We cannot emphasize strongly enough how important the Existence and Uniqueness theorem is for the topological discussion which forms the core of this work. Much of our discussion deals with closed periodic orbits in dynamical systems which exhibit chaotic behavior. To be explicit, we depend heavily on the fact that, in three dimensions, the topological organization of such orbits cannot change under any deformation. In order for the organization to change, one orbit would have to pass through another. This means that at some stage of the deformation, two orbits would pass through the same point in phase space. The existence and uniqueness theorem guarantees that this cannot occur. More specifically, if two closed orbits share a single point, the two orbits must be identical.

6.3 Examples of Dynamical Systems

The archetypical dynamical system is the set of equations representing the Newtonian motion of N independent point particles under their mutual interactions, gravitational or not. In three dimensions, this consists of $n = 6N$ first order coupled ordinary differential equations: three for the coordinates and three for the momenta of each particle. Under the gravitational interaction this system is non Lipschitz: the gravitational potential energy diverges when any pair of particles becomes arbitrarily close.

In the following four subsections we give four examples of dynamical systems. These are four of the most commonly studied dynamical systems. The examples are presented in the historical order in which they were introduced.

In the fifth subsection we give examples of some differential equations which are not equivalent to finite dimensional dynamical systems.

6.3.1 Duffing Equation

The Duffing equation was originally introduced to study the mechanical effects of nonlinearities in nonideal springs. The force due to such a spring was assumed to be a perturbation of the general spring force law $F(x) = -kx$ which retained the symmetry $F(-x) = -F(x)$. The simplest perturbation of this form is $F(x) = -kx - \alpha x^3$ with nonlinear spring 'constant' $k + \alpha x^2$. The spring is "harder" than an ideal spring if $\alpha > 0$, "softer" if $\alpha < 0$. The potential for this nonideal spring force is even: $U(x) = \frac{1}{2}kx^2 + \frac{1}{4}\alpha x^4$. The equations of motion for a mass m attached to a massless nonideal spring, with damping constant γ, are

$$\begin{aligned} \frac{dx}{dt} &= v \\ m\frac{dv}{dt} &= F = -\frac{dU}{dx} - \gamma v \end{aligned} \tag{6.2}$$

These two equations can be combined to a single second order equation in the variable x:

$$\ddot{x} + \gamma\dot{x} + \frac{1}{m}\frac{dU}{dx} = 0 \tag{6.3}$$

In what follows we set $m = 1$ for convenience.

The potential $U(x)$ leads to exciting behavior if we relax the condition that it represents a small perturbation of an ideal spring. That is, we assume the potential may be *un*stable near the origin, but is globally stable. A family of potentials with these properties is

$$A_3 : \qquad U(x) = -\frac{1}{2}\lambda x^2 + \frac{1}{4}x^4 \tag{6.4}$$

Here the parameter λ defines the strength of the instability at the origin. For $\lambda > 0$, the potential has an unstable fixed point at $x = 0$ and two symmetrically distributed stable fixed points at $x = \pm\sqrt{\lambda}$. This potential describes many physical systems of interest: for example, a column under sufficient stress that it buckles (*c.f.*, Fig. 6.1). The dynamics of the system (6.3) are relatively simple: Any initial condition eventually decays to one of the two ground states. However, if the oscillator is periodically driven by including a forcing term of the form $f\cos\omega t$, the two coupled equations of motion become

$$\begin{aligned} \frac{dx}{dt} &= v \\ \frac{dv}{dt} &= -\frac{dU}{dx} - \gamma\dot{x} + f\cos\omega t \end{aligned} \tag{6.5}$$

These two equations can be combined to a second order equation in the single variable x:

$$\ddot{x} + \gamma\dot{x} + x^3 - \lambda x = f\cos\omega t \tag{6.6}$$

This equation for the driven damped Duffing oscillator leads to behavior which is still not completely understood.

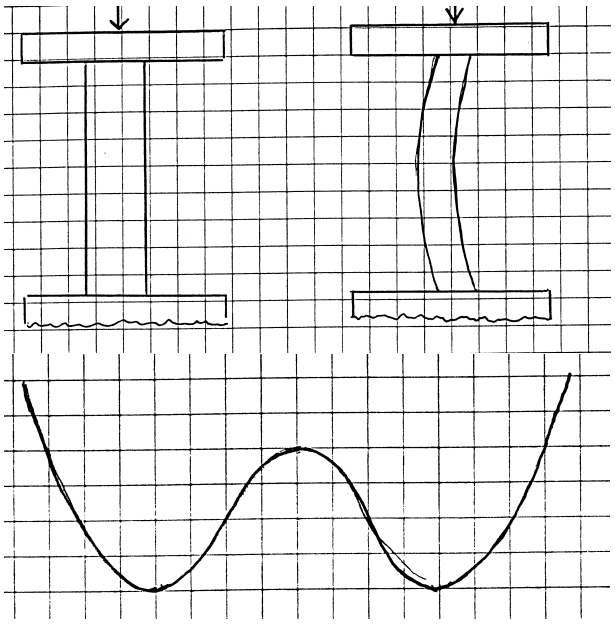

Figure 6.1: Top: A vertical beam under excessive compression deforms to one of two stable equilibrium states. Bottom: The motion of a mass in a double well potential driven by a periodic symmetry-breaking term is described by the Duffing equations (6.6).

6.3.2 van der Pol Equation

The van der Pol equation arises in a natural way when we consider the effect of a nonlinear resistor in a series RLC circuit.

A simple RLC circuit is shown in Fig. 6.2a. If we label the current flowing through the resistor as I_R and the voltage across the resistor as V_R, and similarly for the condensor ($_C$) and inductor ($_L$), then the Kirchoff current and voltage laws impose the following constraints on the currents and voltages in this simple series system:

$$\begin{array}{ccccccc} I_R & = & I_L & = & I_C & & \\ V_R & + & V_L & + & V_C & = & 0 \end{array} \tag{6.7}$$

The dynamics of the circuit is governed by the equations of motion relating currents and voltages in the condensor and inductor

$$\begin{aligned} L\frac{dI_L}{dt} &= V_L \\ C\frac{dV_C}{dt} &= I_C \end{aligned} \tag{6.8}$$

and the constitutive relation for the resistor

$$V_R = f(I_R) \tag{6.9}$$

A linear relation ($V_R = RI_R$, R is the *resistance* of the resistor) is usually assumed. However, interesting dynamics occurs if we can create a resistor which is nonlinear, especially if its linearization in the region of small currents has a negative value: $df(x)/dx < 0$ for $x \simeq 0$). It is convenient to retain the symmetry of $f(x)$, that is $f(-x) = -f(x)$. A convenient choice for the functional form of f is

$$A_2: \qquad f(x) = \frac{1}{3}x^3 - \lambda x \tag{6.10}$$

The dynamical equations of motion are then easily obtained from (6.8). We simplify by setting $L = C = 1$, $I_L = I_C = I_R = x$ and $V_C = y$. Then

$$\begin{aligned} \frac{dx}{dt} &= V_L = -V_C - V_R = -y - f(x) \\ \frac{dy}{dt} &= I_C = x \end{aligned} \tag{6.11}$$

These two equations can be combined to a second order equation in the single variable x:

$$\ddot{x} + (x^2 - \lambda)\dot{x} + x = 0 \tag{6.12}$$

This is one standard form of the time independent van der Pol equation.

In Chapter ?? we will study a periodically driven form of the van der Pol equation. The driving terms can be introduced in two different ways, as shown in Fig. 6.2b. We can place a periodic voltage source $-v\sin\omega_1 t$ in the series circuit

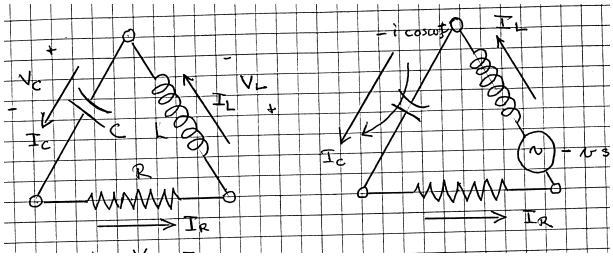

Figure 6.2: (a) Triangular RLC series circuit. (b) Triangular RLC series circuit with periodic forcing terms in the C and L legs.

or put a periodic current $-i\cos\omega_2 t$ through the capacitor. The dynamical equations are

$$\begin{aligned} \frac{dI_L}{dt} &= V_L = -V_C - V_R + v\sin\omega_1 t \\ \frac{dV_C}{dt} &= I_C - i\cos\omega_2 t \end{aligned} \tag{6.13}$$

Employing the same substitutions as before ($x = I_L = I_R = I_C$ and $y = V_C$) we find

$$\begin{aligned} \frac{dx}{dt} &= -y - f(x) + v\sin\omega_1 t \\ \frac{dy}{dt} &= x - i\cos\omega_2 t \end{aligned} \tag{6.14}$$

Once again, these two first order equations in the dynamical variables x and y can be expressed as a single second order equation in one of them:

$$\ddot{x} + (x^2 - \lambda)\dot{x} + x = v\omega_1\cos\omega_1 t + i\cos\omega_2 t \tag{6.15}$$

This equation for the periodically driven van der Pol oscillator also leads to behavior which is still not completely understood.

6.3.3 Lorenz Equations

The Lorenz equations arise as a suitable truncation of the Navier-Stokes equations subject to appropriate boundary conditions.

The physical problem which leads to this set of equations is summarized in Fig. 6.3. This cartoon shows a fluid which is heated from below. When the

transfer of heat to the fluid is low (left), heat is transferred from the bottom to the top by heat conduction alone. The fluid remains at rest. If the heating rate is increased, heat conduction alone is not sufficient to transport the heat rapidly enough from the bottom to the top: the fluid helps out by organizing itself into rolls which help to convey heat from the lower surface to the upper surface (middle). When the heating rate is increased further, the simple organized fluid rolls break up and the behavior appears 'turbulent' (right).

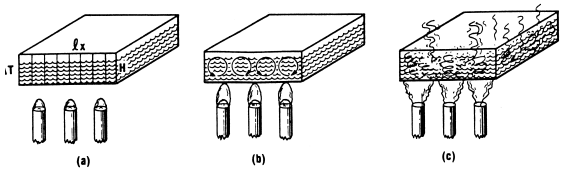

Figure 6.3: (a) At low temperatures, heat is transported by thermal conduction alone. (b) At higher temperatures, the fluid helps out by moving in orderly, self-organized rolls. The rolls may be unchanging in time, may vary periodically, or even chaotically. (c) At very high temperatures the spacially organized roll structures break up into turbulent motion. (Fig. 20.22, p. 563 from CTSE.)

The physics of incompressible fluid motion under thermal stress is described by the Navier-Stokes equations:

$$\begin{aligned} \left(\frac{\partial}{\partial t} + \mathbf{u}\cdot\nabla\right)\mathbf{u} &= \epsilon\mathbf{g}\Delta T - \frac{1}{\rho}\nabla P + \nu\nabla^2\mathbf{u} \\ \left(\frac{\partial}{\partial t} + \mathbf{u}\cdot\nabla\right)T &= \kappa\nabla^2 T \\ \nabla\cdot\mathbf{u} &= 0 \end{aligned} \tag{6.16}$$

The fluid velocity field is $\mathbf{u} = \mathbf{u}(\mathbf{x}) = \mathbf{u}(x, y, z)$ and $T = T(x, y, z)$ is the temperature field. The first equation describes the evolution of the fluid velocity field. The second equation describes the evolution of the temperature field. The third equation is the incompressibility condition. In these equations: ϵ is the coefficient of thermal expansion, $\mathbf{g}$ describes the gravitational force, ΔT is the constant temperature difference imposed between the lower and the upper surface of the fluid, P is the fluid pressure field, ν is the fluid viscosity, and κ is the thermal conduction coefficient.

This problem is simplified by making some assumptions and introducing new variables. First, we introduce a scalar stream function $\psi(x, y, z)$ whose gradient is the velocity field: $\nabla\psi = \mathbf{u}$. We also introduce a function θ which is the difference between the temperature field in the fluid and the temperature field in the static case (Fig. 6.3a): $\theta(x, y, z) = T(x, y, z) - T_{av}$, where T_{av} decreases linearly between the bottom and the top surface. We also assume isotropy in the y direction.

The auxiliary functions obey the equations

$$\begin{aligned} \frac{\partial}{\partial t}\nabla^2\psi &= -\frac{\partial(\psi,\nabla^2\psi)}{\partial(x,z)} + \nu\nabla^4\psi + \epsilon g\frac{\partial\theta}{\partial x} \\ \frac{\partial}{\partial t}\theta &= -\frac{\partial(\psi,\theta)}{\partial(x,z)} + \frac{\Delta T}{H}\frac{\partial\psi}{\partial x} + \kappa\nabla^2\theta \\ \nabla^2\psi &= 0 \end{aligned} \tag{6.17}$$

The boundary conditions on the auxiliary functions $\psi(x,z,t)$ and $\theta(x,z,t)$ for a container of width L (in the x direction) and height H (in the z direction) are that both ψ and $(\partial\theta/\partial x)$ vanish on the boundaries. As a result, Fourier representations of these functions must assume the form

$$\begin{aligned} \psi(x,z,t) &= \sum_{m_1 m_2} A_{m_1 m_2}(t)\sin\frac{m_1\pi x}{L}\sin\frac{m_2\pi z}{H} \\ \theta(x,z,t) &= \sum_{n_1 n_2} B_{n_1 n_2}(t)\cos\frac{n_1\pi x}{L}\sin\frac{n_2\pi z}{H} \end{aligned} \tag{6.18}$$

Here m, n are positive integers, and n_1 can also be zero. These expressions can be substituted into the partial differential equations (6.17) for the auxiliary variables. The time derivatives act on the Fourier coefficients $A_{m_1 m_2}(t)$, $B_{n_1 n_2}(t)$ on the left hand side of the equations (6.17). All spacial derivatives which appear on the right hand side of these equations are easily computed. Integrating out the spacial functions leads to a set of coupled nonlinear ordinary differential equations in which the forcing terms on the right hand side are polynomial functions (at most quadratic) of the Fourier coefficients. The set contains an infinite number (countable) of time-dependent Fourier coefficients.

The usual procedure is to truncate this set of equations by considering only a finite number of terms in the expansion for the two auxiliary functions. Saltzman studied a trunction containing about 20 Fourier coefficients. He found that in many instances all but three coefficients relaxed to zero after sufficiently long time. Lorenz reduced the complexity of the problem by studying a very severe truncation of this problem containing only the three Fourier modes which persisted in Saltzman's simulations. These correspond to the expansions

$$\begin{aligned} \frac{a}{\kappa(1+a^2)}\psi &= \sqrt{2}X\sin\frac{\pi x}{L}\sin\frac{\pi z}{H} \\ \pi\frac{R_a}{R_c}\frac{\theta}{\Delta T} &= \sqrt{2}Y\cos\frac{\pi x}{L}\sin\frac{\pi z}{H} - Z\sin\frac{2\pi z}{H} \end{aligned} \tag{6.19}$$

Here $X \sim A_{11}$, $Y \sim B_{11}$, and $Z \sim B_{02}$. Substituting this ansatz into (6.17) and integrating out the spacial dependence leads to the Lorenz equations for the three Fourier amplitudes X, Y, Z:

$$\begin{aligned} \frac{d}{d\tau}X &= -\sigma X + \sigma Y \\ \frac{d}{d\tau}Y &= rX - Y - XZ \end{aligned} \tag{6.20}$$

$$\frac{d}{d\tau}Z = -bZ + XY$$

The parameters which appear in this set of equations are $a = H/L$, $R_a = \epsilon g H^4(\Delta T/H)/(\kappa\nu)$, $R_c = \pi^4(1+a^2)^3/a^2$, $r = R_a/R_c$, $\sigma = \nu/\kappa$, $b = 4/(1+a^2)$, and $\tau = (\pi/H)^2(1+a^2)\kappa t$.

The equations (6.20) are known as the Lorenz equations. These are the equations in which the property of 'sensitivity to initial conditions' was first studied in detail.

6.3.4 Rössler Equations

The Lorenz equations possess two nonlinearities ($-XZ$ in the second equation and $+XY$ in the third) and exhibit three fixed points. Rössler felt that there should be a simpler set of equations which exhibits the same generic behavior: sensitivity to initial conditions and chaotic behavior. 'Simpler' meant fewer nonlinear terms and a smaller number of fixed points. Accordingly, he set out to construct a simpler set, in the spirit of Dirac setting out to find a simpler version of the equation for an electron by factoring the Klein-Gordan equation into two 'simpler' equations.

Rössler began by considering motion in the neighborhood of an unstable focus in the x-y plane. Such motion can occur in a two dimensional dynamical system of the form

$$\begin{aligned} \dot{x} &= -y \\ \dot{y} &= x + ay \end{aligned} \tag{6.21}$$

He then added a term which forces the motion out of the x-y plane when it gets too far away from the origin. This involves an equation of motion for the z-direction. He chose the simple form $\dot{z} = b + z(x - c)$. Here b is small and positive, causing the value of z to increase slowly when z and x are small. When x becomes larger than c, $\dot{z}$ becomes large and the z coordinate suddenly "blasts off" from the x-y plane. Finally, one more term was added to the original two-dimensional dynamical system which forces x to suddenly decrease when z becomes large. In final form, the Rössler equations are

$$\begin{aligned} \dot{x} &= -y - z \\ \dot{y} &= x + ay \\ \dot{z} &= b + z(x - c) \end{aligned} \tag{6.22}$$

These equations are simpler than the Lorenz equations in the sense that they contain only one nonlinearity (zx in the third equation) and possess only two fixed points.

The Rössler equations have been widely studied over a broad range of control parameter values (a, b, c). Although these equations were not motivated through consideration of some physical problem (as opposed to the Duffing, van der Pol,

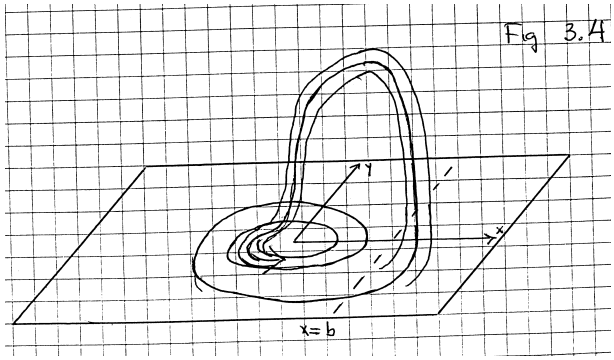

Figure 6.4: The flow dynamics generated by the Rössler equations is represented by this cartoon.

and Lorenz equations), the behavior of these equations serves to model a wide variety of real physical systems.

A cartoon representing the dynamics of the Rössler system is presented in Fig. 6.4.

6.3.5 Examples of non Dynamical Systems

Many physical systems can be described, or at least reasonably well approximated by, sets of ordinary differential equations. Lest we leave the impression that all of physics is described by dynamical systems, we present two examples which do not fall under this rubric.

Equation with non-Lipschitz Forcing Terms.

The equation

$$\frac{dx}{dt} = \sqrt{2x} \tag{6.23}$$

has a forcing term ($\sqrt{2x}$) which is non-Lipschitz. Its derivative, $1/\sqrt{2x}$, is not bounded in the neighborhood of the origin. As a result, the Existence and Uniqueness theorem is not applicable. To make this point clear, this equation has two distinct solutions through $x_0 = 0$. One solution is $x(t) = 0$, $-\infty \leq t \leq +\infty$. The other solution is $x(t) = \frac{1}{2}t^2$, $-\infty \leq t \leq +\infty$.

Stochastic Differential Equations

Partial differential equations are generally more difficult to handle than ordinary differential equations. For this reason a large industry has grown up around the problem of reducing partial to ordinary differential equations.

We have illustrated one approach to this reduction in our discussion of the Lorenz equations. This procedure is useful for partial differential equations of evolution type: $\partial u/\partial t = F(u, \nabla u, \cdots, t)$. The dependent fields are expanded in terms of a complete set of orthogonal spacial modes, $\Phi_\mu(x)$, which satisfy the appropriate boundary conditions. These expressions are inserted into the partial differential equations, and the spacial dependence is integrated out. This results in a set of coupled ordinary differential equations. There is one equation for each amplitude. The source terms consist of polynomial products involving the amplitudes and numerical coefficients which are Clebsch-Gordan coefficients for the orthogonal modes. If the function $F(*)$ contains quadratic, cubic, ... nonlinearities in the dependent fields, the source terms in the projected coupled ordinary differential equations will contain only quadratic, cubic, ... products of the amplitudes. For example, the Navier-Stokes equations contain only quadratic nonlinearities. Therefore any Galerkin projection of these equations will contain only quadratic couplings involving the mode amplitudes, no matter what complete set of modes is used for the expansion of the dependent functions.

Suppose, to be specific, that a partial differential equation contains only quadratic nonlinearities. We assume that the dependent fields have an expansion

$$u(x,t) = \sum_i x_i(t)\Phi_i(x) + \sum_\alpha y_\alpha(t)\Phi_\alpha(x) \tag{6.24}$$

where $i = 1, 2, \cdots, n$ and $\alpha = n+1, \cdots$. We assume that the modes numbered 1 through n are the most important modes under the conditions specified. Then the projection procedure outlined above will lead to a set of equations for the mode amplitudes x_i of the form

$$\frac{dx_i}{dt} = A_i + A_{i,j}x_j + A_{i,\beta}y_\beta + A_{i,jk}x_jx_k + A_{i,j\gamma}x_jy_\gamma + A_{i,\beta\gamma}y_\beta y_\gamma \tag{6.25}$$

A similar equation can be written for the dy_α/dt.

This set of equations is not closed. The evolution of the x_i depend on the time dependence of the y_α, which are not known. The $y_\alpha(t)$ dependence can be 'removed' by writing these equations in the form

$$\frac{dx_i}{dt} = A_i + A_{i,j}x_j + A_{i,jk}x_jx_k + \epsilon_i(t) + \epsilon_{i,j}(t)x_j \tag{6.26}$$

The two time dependent functions are

$$\begin{aligned} \epsilon_i(t) &= \sum_\beta A_{i,\beta}y_\beta + \sum_{\beta\gamma} A_{i,\beta\gamma}y_\beta y_\gamma \\ \epsilon_{i,j}(t) &= \sum_\gamma A_{i,j\gamma}y_\gamma \end{aligned} \tag{6.27}$$

If we are careful (or lucky), the time dependent functions $\epsilon_i(t)$ and $\epsilon_{i,j}(t)$ will not have large amplitudes, and we might even be able to say something about their properties (mean values, moments, correlation functions).

In many cases, the function $\epsilon_i(t)$ is treated as an additive noise term and the functions $\epsilon_{i,j}(t)$ are treated as multiplicative noise terms in the equation for x_i. Equations of the type (6.26) are called stochastic differential equations.

Remark: Two distinct approaches exist for introducing normal modes $\Phi_\mu(x)$ into decompositions of type (6.24). For purely theoretical analyses, the normal modes $\Phi_\mu(x)$ are usually taken as some convenient set in which to analyze the appropriate equations - for example, Fourier modes. For analyses which involve observational data, empirical modes are very often constructed by processing the data. A much used procedure involves constructing a set of orthogonal modes using a singular value decomposition.

6.3.6 Additional Observations

We can draw a number of general observations from the specific properties exhibited by the examples discussed above.

Nonautonomous → Autonomous Form: The Lorenz equations (6.20) and the Rössler equations (6.22) are autonomous. The periodically driven Duffing equations (6.5) and the periodically driven van der Pol equations (6.14) are nonautonomous.

All periodically driven dynamical systems are nonautonomous. If the driving terms are of the form $\sin\omega t$, $\cos\omega t$, the nonautonomous set of equations can be replaced by an autonomous dynamical system of higher dimension by adjoining to the original set the following equations

$$\begin{aligned} \dot{r}_1 &= -\omega r_2 \\ \dot{r}_2 &= +\omega r_1 \end{aligned} \tag{6.28}$$

and then replacing $\sin\omega t$, $\cos\omega t$ by r_1, r_2 wherever they occur. When this is done, the source terms for the Duffing and van der Pol equations are low degree polynomials in the appropriate variables.

Structure of Phase Space: The phase spaces for the Lorenz and Rössler systems are R^3. The phase spaces for the periodically driven Duffing and van der Pol oscillators are also three dimensional but topologically different: they are $R^2 \times S^1$. The S^1 part of the phase space refers to the periodic driving term.

Symmetry: Dynamical systems sometimes exhibit symmetries. When this occurs, the symmetries impose constraints on the behavior. These constraints often simplify the discussion of the properties of these systems.

To be more explicit, the scalar function $A_2 : f(x) = \frac{1}{3}x^3 - \lambda x$ which appears in the van der Pol equations and the scalar function $A_3 : U(x) = \frac{1}{4}x^4 - \frac{1}{2}\lambda x^2$ which appears in the Duffing equations both have a symmetry under the group action $x \to -x$. These symmetries propagate to the periodically driven equations, as follows. If either i or v is zero in the driven van der Pol equation (6.14), then the equations are unchanged ("equivariant") under $(x, y, t) \to (-x, -y, t + \frac{1}{2}T)$, where T is the period of the driving term. Similarly, the Duffing equations (6.5) are equivariant under the same transformation

$(x, y, t) \to (-x, -y, t + \frac{1}{2}T)$. In both cases, the symmetry is easily visualized as a symmetry in the phase space $R^2(x, y) \times S^1(\theta) \to R^2(-x, -y) \times S^1(\theta + \pi)$.

The Lorenz equations also exhibit a symmetry. They are equivariant under $(X, Y, Z) \to (-X, -Y, +Z)$. This symmetry is easily visualized as a rotation through 180° about the Z axis in the phase space. The origin of this symmetry lies in the Navier-Stokes equations. For the boundary conditions chosen, these equations are unchanged under the real physical space coordinate transformation $(x, z) \to (L - x, z)$. Under this transformation the potentials satisfy

$$\begin{aligned} \psi(x, z, t) &= -\psi(L - x, z, t) \\ \theta(x, z, t) &= +\theta(L - x, z, t) \end{aligned} \tag{6.29}$$

This symmetry requires the following symmetries on the Fourier coefficients: $A_{m_1 m_2} \to (-)^{m_1} A_{m_1 m_2}$ and $B_{n_1 n_2} \to (-)^{n_1} B_{n_1 n_2}$. All truncations of the Navier Stokes equations for this geometry will exhibit this two-fold symmetry.

Singularities: In the work that follows, we will show that singularities play an important role in the creation and classification of strange attractors. We have already encountered two of the simplest singularities: the fold and the cusp. The function $f(x, \lambda) = \frac{1}{3}x^3 - \lambda x$ is a one parameter family of functions which contains a singularity ($d^2 f/dx^2 = 0$ when $df/dx = 0$) at $\lambda = 0$. This family of functions contains the fold singularity x^3 and is denoted A_2. The function $U(x, \lambda) = \frac{1}{4}x^4 - \frac{1}{2}\lambda x^2$ belongs to a two parameter family of functions which contains the cusp singularity x^4, which is denoted A_3. The second parameter (b) in this family, $U(x, \lambda) = \frac{1}{4}x^4 - \frac{1}{2}\lambda x^2 + bx$, is restricted to be zero by symmetry considerations.

Singularities will be encountered in several different ways in our studies of dynamical systems which can exhibit chaotic behavior. For example, we will see in Sec. 6.5.3 that the fixed points of the Rössler equations can experience a fold singularity (A_2) and those of the Lorenz equations can experience a symmetry restricted cusp singularity (A_3) as control parameters are varied.

n^{th} Order Equations: Ordinary differential equations have also been represented by a scalar constraint on the first n derivatives of a single variable:

$$G(y, y^{(1)}, y^{(2)}, \cdots, y^{(n)}) = 0 \tag{6.30}$$

In this expression, $y = y^{(0)}$ and $y^{(i+1)} = dy^{(i)}/dt$. The scalar equation (6.30) represents a surface in the $n + 1$ dimensional space whose coordinates are the state variable y and its first n derivatives. This is an n^{th} order equation.

If the derivative $y^{(n)}$ occurs linearly in (6.30), so that $G(*) = y^{(n)} - g(y, y^{(1)}, \cdots, y^{(n-1)})$ then this equation can be written as a dynamical system by defining n variables $x_i = y^{(i-1)}$, with $x_1 = y$, so that

$$\begin{aligned} \frac{dx_1}{dt} &= x_2 \\ \frac{dx_2}{dt} &= x_3 \\ &\vdots \end{aligned} \tag{6.31}$$

$$\begin{aligned} \frac{dx_{n-1}}{dt} &= x_n \\ \frac{dx_n}{dt} &= g(x_1, x_2, \cdots, x_n) \end{aligned}$$

The equations (6.3) and (6.12) for the undriven Duffing and van der Pol oscillators have the form (6.30) of second order equations in a single variable.

If the function G in (6.30) is explicitly time dependent, the corresponding dynamical system is nonautonomous. The first remark in this subsection can then be used to construct a simple time-independent surface of the form (6.30) in a higher dimensional space. This is possible for periodically driven dynamical systems.

Vector Fields: A dynamical system defines a vector field on its phase space. The following intuitive argument describes one way to make this association.

Assume that some function $P(x,t)$, $x \in R^n$, is defined on the phase space. This could represent some probability distribution, for example. If the evolution is due entirely to the dynamical evolution of the points in the phase space, then $P(x,t) = P(x(t))$. The time evolution is then

$$\begin{aligned} P(x', t+dt) &= P(x(t+dt)) \\ &= P(x_i(t) + dt\dot{x}_i(t)) \\ &= P(x(t)) + dt\dot{x}_i(t)\frac{\partial}{\partial x_i}P(x) \end{aligned} \tag{6.32}$$

The differential operator $V = \frac{dx_i}{dt}\frac{\partial}{\partial x_i}$ is the vector field associated with the dynamical system. This can be expressed in terms of the source functions using $\dot{x}_i = F_i(x)$ as follows: $V = F_i(x)\frac{\partial}{\partial x_i}$.

6.4 Change of Variables

Physical results should be independent of the mathematics used to describe these results. To put this another way: our results should be independent of the coordinate system we choose to describe these results. This means that we should be free to choose different coordinate sytems without the risk of altering our predictions. In particular, one of the virtues of having many coordinate systems in which to perform calculations is that we are free to choose the coordinate system which simplifies, to the greatest extent possible, the computational difficulties.

6.4.1 Diffeomorphisms

Different but equivalent coordinate systems for sets of ordinary differential equations are related by diffeomorphisms.

Definition: A diffeomorphism from a space U to a space V is a $1 \leftrightarrow 1$ map which is onto and differentiable, and whose inverse is also differentiable.

Example: A nonsingular linear transformation $x_i \to x_i' = \sum_j A_i^j x_j$ is a diffeomorphism.

Remark: Two n-dimensional dynamical systems which are related by a diffeomorphism are equivalent. That is, any property of one has a counterpart in the other dynamical system.

Remark: For most of our purposes, $U = V = R^3$.

Remark: It is sometimes useful to consider mappings which are *local* but not *global* diffeomorphisms. An example of a local diffeomorphism is the map $(x, y, z) \to (u, v, w) = (x^2 - y^2, 2xy, z)$. This mapping is not 1-1, but 2-1 for all points off the z-axis. The Jacobian of this transformation is singular on the z-axis. Open subsets $U \subset R^3$ and $V \subset R^3$ exist on which this map is a local diffeomorphism. Dynamical systems on two subsets which are related by this map are *locally* equivalent but not *globally* equivalent. We will discuss the relation between dynamical systems which are everywhere locally equivalent, but not globally equivalent, in Chapter ??.

6.4.2 Examples

In this subsection we will consider three examples of changes of variables. The first two involve transformations from the original set of variables $(x_1, x_2, \cdots, x_n)$ to a new set of variables $(u_1, u_2, \cdots, u_n)$ which are differentially related to each other: $du_i/dt = u_{i+1}$, $i = 1, 2, \cdots, n-1$. In the first example the change of variables is a diffeomorphism; in the second it is not. In the third example, the change of variables is a local but not a global diffeomorphism.

Example 1: The general procedure for transforming a dynamical system $\dot{x}_i = F_i(x)$ from the original coordinates to a new set of differential coordinates $u_i = u^{(i-1)}$ is as follows.

1. Choose a function $\zeta = \zeta(x)$ of the original set of coordinates.
2. Define the new coordinate by $u_1 = \zeta(x)$.
3. Construct the next component using
$$u_2 = \frac{du_1}{dt} = \frac{d\zeta(x)}{dt} = \frac{dx_i}{dt}\frac{\partial}{\partial x_i}\zeta(x) = \left(F_i \frac{\partial}{\partial x_i}\right)\zeta(x) \tag{6.33}$$
4. Iterate this procedure, using the operator $F_i\partial_i$, to construct $u_3, \cdots, u_n$, and finally $du_n/dt = g(x_1, \cdots, x_n)$.
5. Express the old coordinates x_i in terms of the new coordinates u_j.
6. Substitute the new coordinates into the last equation, to find
$$\begin{aligned} \dot{u}_1 &= u_2 \\ \dot{u}_2 &= u_3 \\ &\vdots \end{aligned} \tag{6.34}$$

$$\begin{aligned} \dot{u}_{n-1} &= u_n \\ \dot{u}_n &= g(u_1, \cdots, u_n) \end{aligned}$$

We provide a simple illustration using the Rössler equations (6.22). We define $(x_1, x_2, x_3) = (x, y, z)$ and $(u_1, u_2, u_3) = (u, v, w)$, and choose $\zeta = y$. Then

$$\begin{aligned} u &= y \\ v &= x + ay \\ w &= ax + (a^2 - 1)y - z \\ \frac{dw}{dt} &= a(-y - z) + (a^2 - 1)(x + ay) - [b + z(x - c)] \end{aligned} \tag{6.35}$$

The first three equations are easily inverted

$$\begin{aligned} y &= u \\ x &= v - au \\ z &= -u + av - w \end{aligned} \tag{6.36}$$

Since the transformation between the original and new set of coordinates is linear with determinant $+1$, it is a global diffeomorphism. In the new coordinate system the dynamical system equations are

$$\begin{aligned} \frac{du}{dt} &= v \\ \frac{dv}{dt} &= w \\ \frac{dw}{dt} &= g(u, v, w) = (a - c)u + (ac - a - 1)v + (a - c)w - b \\ &\qquad -(v - au)(-u + av - w) \end{aligned} \tag{6.37}$$

Example 2: We perform the same calculation now for the Lorenz set of equations (6.20), choosing $\zeta(x, y, z) = x$. Proceeding as above, we find

$$\begin{aligned} x &= u \\ y &= u + (1/\sigma)v \\ z &= r - 1 - [w + (\sigma + 1)v]/(\sigma u) \end{aligned} \tag{6.38}$$

This transformation is singular, with determinant $1/(\sigma^2 u)$. The equations of motion have the form (6.37), where the function $g(u, v, w)$ is now singular:

$$\begin{aligned} g(u, v, w) &= g_0(u, v, w) + g_{-1}(u, v, w)/u \\ g_0(u, v, w) &= \sigma b(r - 1)u - (\sigma + 1)bv - (\sigma + b + 1)w - u^2 v - \sigma u^3 \\ g_{-1}(u, v, w) &= (\sigma + 1 + w)v \end{aligned} \tag{6.39}$$

In this form, the source term on the right hand side does not obey a Lipschitz condition, so that the fundamental theorem does not apply to trajectories which approach the $u = 0$ plane.

Example 3: In this example we again carry out a change of variables on the Lorenz equations (6.20). These equations are equivariant (unchanged) under a group consisting of two elements: the identity and a rotation by π radians about the z-axis: $R_z(\pi)$. We choose a change of variables which maps each pair of symmetry related points (x, y, z) and $(-x, -y, +z)$ into the same point: $(u, v, w) = (x^2 - y^2, 2xy, z)$. The dynamical system equations in the new coordinate system are easily expressed in terms of the Jacobian of the transformation: $du_i/dt = (\partial u_i/\partial x_j)(dx_j/dt)$. This is explicitly

$$\frac{d}{dt}\begin{bmatrix} u \\ v \\ w \end{bmatrix} = \begin{bmatrix} 2x & -2y & 0 \\ 2y & 2x & 0 \\ 0 & 0 & 1 \end{bmatrix} \begin{bmatrix} -\sigma x + \sigma y \\ rx - y - xz \\ -bz + xy \end{bmatrix}$$

$$= \begin{bmatrix} -(\sigma+1)u + (\sigma - r + w)v + (1-\sigma)\rho \\ (r - \sigma - w)u - (1+\sigma)v + (r + \sigma - w)\rho \\ -bw + v/2 \end{bmatrix} \tag{6.40}$$

where $\rho = \sqrt{u^2 + v^2}$. This last equation no longer possesses a symmetry. It is a $2 \to 1$ image of the original equations, which have a two-fold symmetry.

6.4.3 Structure Theory

As the examples above show, the form of a dynamical system can change remarkably under a diffeomorphism. It would be useful to have a method for simplifying dynamical systems. Suppose it is possible to find coordinates $y_1, y_2, \cdots, y_{n_1}$ and $z_1, z_2, \cdots, z_{n_2}$, $n_1 + n_2 = n$, so that the n dimensional dynamical system (6.1) can be written in the form

$$\begin{aligned} \frac{dy_i}{dt} &= G_i(y, z) \qquad i = 1, 2, \cdots, n_1 \\ \frac{dz_j}{dt} &= H_j(-, z) \qquad j = 1, 2, \cdots, n_2 \end{aligned} \tag{6.41}$$

In this expression, $H_j(-, z)$ means that the functions H_j do not depend on the variables y. Then the second set of n_2 equations depends on the n_2 variables z_j alone. This dynamical subsystem can then be integrated independently of the y variables. The explicit solutions can be used as time-dependent driving terms in the first set of n_1 equations which depend on the n_1 variables y: $dy_i/dt = G_i(y, z(t)) \to G_i(y, t)$. The phase space for the z subsystem is R^{n_2}; the phase space for the full dynamical system is $R^n \sim R^{n_1} \times R^{n_2}$.

A dynamical system with the form described in (6.41) is called *reducible*.

If reducibility of a dynamical system simplifies its treatment, complete reducibility simplifies the treatment even further. A dynamical system (6.1) is

fully reducible (completely reducible) if it is possible to find a diffeomorphism $x \to (y, z)$ so that the equations of motion assume the form

$$\begin{aligned} \frac{dy_i}{dt} &= G_i(y, -) \qquad i = 1, 2, \cdots, n_1 \\ \frac{dz_j}{dt} &= H_j(-, z) \qquad j = 1, 2, \cdots, n_2 \end{aligned} \tag{6.42}$$

In this case, each of the two dynamical subsystems evolves independently of the other.

A dynamical system is *irreducible* if there is no diffeomorphism which maps it to the form (6.41).

To date, the full power of transformation theory has not been exploited to simplify dynamical systems theory. Specifically, it would be very nice to have some kind of algorithm (analogous to Ado's algorithm in the theory of Lie algebras) which identifies irreducible dynamical systems. Specifically, the algorithm should do three things. First, answer the question: "Is this dynamical system reducible?" If the answer to the first question is "Yes", then the algorithm should provide a method for constructing the diffeomorphism which effects the transformation to reduced form. Finally, the algorithm should carry out this transformation and display the reduced dynamical system equations.

Example: The driven Duffing equations can be written in the reducible form

$$\begin{aligned} \frac{dx}{dt} &= v \\ \frac{dv}{dt} &= \lambda x - x^3 - \gamma v + f r_1 \\ \frac{dr_1}{dt} &= -\omega r_2 \\ \frac{dr_2}{dt} &= +\omega r_1 \end{aligned} \tag{6.43}$$

More generally, all periodically driven dynamical systems are equivalent to reducible autonomous systems.

Remark: Chaotically driven nonautonomous dynamical systems can be treated similarly. If the chaotic driving terms $z_1, z_2, \cdots, z_{n_2}$ appear in polynomial coupling terms in the original n_1-dimensional dynamical system, then an n_2-dimensional dynamical system generating these terms can be adjoined to the original nonautonomous dynamical system, and the time-dependent terms replaced by functions of the variables z. The resulting $n = n_1 + n_2$-dimensional dynamical system is autonomous and reducible.

Remark: The algorithm for reducibility should have a topological component. For example, the phase space for the Rössler attractor (the dynamics generated by equations (6.22) for certain ranges of the control parameter values) is $R^2 \times S^1$. This strongly suggests that it might be possible to find a coordinate system (a diffeomorphism) in which the Rössler equations assume reducible form. This is currently an open question.

6.5 Fixed Points

The global organization of a dynamical system $\dot{x}_i = F_i(x;c)$ is governed to a large extent by the number, distribution, and stability of its fixed points. The same is true of a map $x'_i = f_i(x)$.

6.5.1 Dependence on Topology of Phase Space

There is a strong relation between the fixed points of a dynamical system, the topological structure of its phase space, and the symmetry of the dynamical system.

If the phase space of an n-dimensional dynamical system has the form $R^{n-1} \times S^1$, the dynamical system has no fixed points. This is the case for the periodically driven Duffing and van der Pol oscillators. The best that can be done is to look for critical points of particular functions (*e.g.*, $U(x), f(x)$) in the constant θ slices of S^1.

If the dynamical system has symmetry, then fixed points fall into classes. A simple example is provided by the Lorenz system, which possesses a two-fold rotation symmetry about the Z axis. In this case, fixed points can exist on the symmetry axis or off the axis. Those which occur off the symmetry axis must occur in symmetry-related pairs. In general, if G is the symmetry group of the dynamical system and p is a fixed point which is invariant under the action of the subgroup $H \subset G$, then p will occur in a multiplet of order $|G|/|H|$, where $|G|$ is the order of G. The *partners* of p are the points in the *orbit* of p under G, or more economically under the quotient (*coset*) G/H. For the Lorenz equations there is one fixed point on the symmetry axis and a symmetry related pair of fixed points off the symmetry axis.

When the phase space is R^n and the dynamical system possess no particular symmetry, then algorithms exist for locating the fixed points of autonomous dynamical systems whose source terms are polynomials in the state variables.

6.5.2 How to Find Fixed Points in R^n

The fixed points of a dynamical system are located by solving the simultaneous nonlinear equations $F_i(x;c) = 0$. Typically, n equations in n phase space variables will have only isolated solutions. The number of solutions will be finite if each of the functions $F_i(x;c)$ is a polynomial of finite degree in the n state variables x_i.

Often the fixed points of a dynamical system can be located by the brute strength approach favored by physicists. For example, the fixed points of the Lorenz system can be obtained using lower algebra. However, it would be comforting to know that more sophisticated methods are available.

The study of solution sets of algebraic equations is the province of algebraic geometry (O'Shea et al). A number of powerful computer programs have been developed to implement algorithms for locating the zeroes of sets of algebraic

equations. We illustrate in Fig. 6.5 how one of these algorithms is used in the widely available package Maple.

First, the Maple package *grobner* is loaded with the command $with(grobner)$;. The output list ($[finduni, \cdots, spoly]$) indicates the programs which are implemented in this package. Then the three polynomial equations which define (:=) the Lorenz equations are input without echoes(:), and collected as an array $F1$ (Maple is case sensitive) with echo(;). The variables $[x, y, z]$ are also collected into an array X. The two arrays, $F1$ and X, are arguments for the *gbasis* routine, which computes the Gröbner basis for these functions. Finally, the routine *gsolve* is called. The output is the set of roots of the simultaneous polynomial equations. Equivalently, it is the set of fixed points of the Lorenz flow.

Here is how to read the output. The roots consist of two sets. One set is $[x, y, z]$, which is to be read $x = 0, y = 0, z = 0$. The other set is $[x - y, y^2 + b - br, -r + 1 + z]$. It is convenient to read these equations from right to left. Thus, in the second set, $z + 1 - r = 0$, then $y^2 + b - br = 0$, which has two solutions, and then $x - y = 0$, which means that for each of the two solutions $y_\pm$, $x = y$.

$with(grobner)$;
$[finduni, finite, gbasis, gsolve, leadmon, normalf, solvable, spoly]$
$> f1 := -sigma * x + sigma * y :$
$> f2 := r * x - y - x * z :$
$> f3 := -b * z + x * y :$
$> F1 := [f1, f2, f3];$
$F1 := [-\sigma x + \sigma y, rx - y - xz, -bz + xy]$
$> X := [x, y, z] :$
$> gbasis(F1, X);$
$[x - y, y^2 - bz, yz + (1 - r)y, z^2 + (1 - r)z]$
$> gsolve(F1, X);$
$[[x, y, z], [x - y, y^2 + b - br, -r + 1 + z]]$

Figure 6.5: This Maple worksheet computes the fixed points of the Lorenz equations.

Although the fixed points of the Lorenz equations can easily be found by hand, such is not the case for more formidable sets of nonlinear polynomial equations. The procedure described here will *always* provide *all* the fixed points of such a dynamical system or map. However, this procedure may take a while for large sets of polynomial equations.

6.5.3 Bifurcations of Fixed Points

The number of fixed points that a dynamical system has is an invariant. This number remains fixed as the control parameters are varied, if one counts their degeneracy. However, the number of *real* fixed points generally depends on the control parameter values, and is not invariant.

The values of the control parameters at which the number of real critical points changes is called the *bifurcation set*. As one passes transversally through the bifurcation set, two critical points with complex conjugate coordinate values scatter off each other to become real critical points.

We illustrate these ideas with two examples.

Example 1: The critical points of the Rössler system (6.22) are given by $z = -y$, $x = -ay$, where y satisfies $ay^2 + cy + b = 0$. The two solutions are $y_\pm = -\frac{c}{2a} \pm \sqrt{(\frac{c}{2a})^2 - \frac{b}{a}}$. The solutions are

Real			> 0
Degenerate	if	$c^2 - 4ab$	$= 0$
Complex			< 0

The bifurcation set in control parameter space is the two dimensional surface $c^2 - 4ab = 0$.

Example 2: The three critical points for the Lorenz system were computed in Fig. 6.5. There is always one real critical point at $(x, y, z) = (0, 0, 0)$. The other two critical points have real coordinate $z = r-1$. The x- and y-coordinates are imaginary if $r < 1$, real if $r > 1$. There is a three-fold degeneracy of the critical points for $r = 1$. The bifurcation from one to three real critical points occurs as the two dimensional surface $r = 1$ in the control parameter space (σ, b, r) is traversed.

Remark: The real fixed points of the Rössler and Lorenz equations lie on one dimensional curves in phase space. These curves are given parametrically as follows:

$$\begin{array}{lrcl} \text{Rössler} & (x, y, z) & = & (\frac{c}{2} - as, -\frac{c}{2a} + s, +\frac{c}{2a} - s) \\ \text{Lorenz} & (x, y, z) & = & (s, s, s^2/b) \end{array}$$

with $-\infty < s < +\infty$. If all the real fixed points of a dynamical system lie on a one-dimensional curve, the dynamical system has rank one. More generally, if all the real fixed points of a dynamical system lie on a surface of minimal dimension r, the dynamical system has *rank r*. The rank of a dynamical system can be determined by identifying the bifurcation which takes place when all the critical points are degenerate. The rank and number of real critical points are important invariants of a dynamical system. They provide a partial classification for dynamical systems. The Rössler and Lorenz systems are of type A_2 and A_3, since their real critical points arise through fold and cusp type bifurcations.

Remark: It is useful to choose a coordinate system which emphasizes the rank of a dynamical system. For the Lorenz system, such a coordinate system (u, v, w) has the property that all critical points lie on the u axis $(u, v = 0, w = 0)$. The following diffeomorphism

$$\begin{array}{rcll} u & = & \alpha x + \beta y & \alpha + \beta = 1 \\ v & = & x - y & \\ w & = & bz - xy & \end{array} \tag{6.44}$$

brings the Lorenz system to the following form

$$\begin{aligned}
\dot{u} &= \beta(r-1)u - [\alpha(\alpha\sigma-\beta)+\beta(\alpha\sigma-\beta r)]\,v - \\
&\qquad (\beta/b)(u+\beta v)\,[w+(u+\beta v)(u-\alpha v)] \\
\dot{v} &= -(r-1)u - (\sigma+\alpha+\beta r)v + \\
&\qquad (1/b)(u+\beta v)\,[w+(u+\beta v)(u-\alpha v)] \\
\dot{w} &= -bw - r(u+\beta v)^2 - \sigma(u-\alpha v)^2 + (\sigma+1)(u+\beta v)(u-\alpha v) + \\
&\qquad (u+\beta v)^2\,[w+(u+\beta v)(u-\alpha v)]
\end{aligned} \tag{6.45}$$

This set of equations remains invariant under the two-fold rotation $R_z(\pi)$: $(u,v,w)\to(-u,-v,+w)$. Its three fixed points lie on the u axis $v=w=0$ and satisfy $(r-1)u-(1/b)u^3=0$. If we choose $\alpha=1/(\sigma+1)$, $\beta=\sigma/(\sigma+1)$, then the linear part of this equation is

$$\frac{d}{dt}\begin{bmatrix} u \\ v \\ w \end{bmatrix} = \begin{bmatrix} \frac{\sigma(r-1)}{\sigma+1} & \frac{\sigma^2(r-1)}{\sigma+1} & 0 \\ -(r-1) & -\sigma-\frac{\sigma r+1}{\sigma+1} & 0 \\ 0 & 0 & -b \end{bmatrix}\begin{bmatrix} u \\ v \\ w \end{bmatrix} \tag{6.46}$$

On the bifurcation set $r-1=0$ this matrix is diagonal, with two negative and one vanishing eigenvalue. The two new fixed points (real nonzero solutions of $(r-1)u-(1/b)u^3=0$ for $r>1$) bifurcate along the u axis. The transformation (6.44) with $\alpha=1/(\sigma+1)$, $\beta=\sigma/(\sigma+1)$ maps to the center manifold $v=w=0$ at the bifurcation $r-1=0$.

6.5.4 Stability of Fixed Points

Once the fixed points of a flow have been located, it is a relatively simple matter to determine their stability.

The flow in the neighborhood of a fixed point can be determined by linearizing the system in the usual way. We write $x(t)=x^*+\delta x$. Then

$$\begin{aligned}
\frac{d}{dt}(x^*+\delta x)_i &= F_i(x^*+\delta x, c) \\
\frac{d\delta x_i}{dt} &= \left.\frac{\partial F_i(x,c)}{\partial x_j}\right|_{x^*}\delta x_j
\end{aligned} \tag{6.47}$$

Stability of motion in the neighborhhod of the fixed point is determined by the eigenvalues $\lambda_i(c)$ of the stability matrix $\partial F_i(x^*,c)/\partial x_j$. Motion relaxes to the fixed point if all the eigenvalues of this matrix have negative real part. The motion is unstable in k directions if k eigenvalues have positive real part. If one or more eigenvalues have zero real part, then under weak conditions, a bifurcation is about to take place as the control parameters c are swept from $c-\delta c$ to $c+\delta c$.

Example: The Jacobian of the Lorenz flow is

$$J = \begin{bmatrix} -\sigma & \sigma & 0 \\ r-z & -1 & -x \\ y & x & -b \end{bmatrix} \tag{6.48}$$

The Jacobian matrix at the fixed point $(x, y, z) = (0, 0, 0)$ on the symmetry axis is simple to evaluate. The eigenvalues and eigenvectors are

$$\begin{array}{ll} \text{eigenvalue} & \text{eigenvector} \\ \lambda_+ & (\sigma, \sigma + \lambda_+, 0) \\ \lambda_- & (\sigma, \sigma + \lambda_-, 0) \\ -b & (0, 0, 1) \end{array} \tag{6.49}$$

where $\lambda_\pm = -\frac{1}{2}(\sigma+1) \pm \sqrt{(\frac{1}{2}(\sigma+1)^2 + \sigma(r-1)}$. For $\sigma, b > 0$, the two eigenvalues λ_- and $-b$ are negative. The third eigenvalue, λ_+, is negative for $r < 1$ and positive for $r > 1$. For $\sigma, b > 0$, this fixed point is stable for $r < 1$ and unstable in one direction for $r > 1$. At $r = 1$ its stablity is determined by including higher order terms in the 'linearized' equations of motion. However, stability is of less interest than the bifurcation which occurs as r passes through $r = 1$. The bifurcation takes place along the eigenvector whose eigenvalue is λ_+ and is of type A_3 (cusp). These two new real fixed points are both stable, by general arguments of topological type.

Similar calculations can be carried out on the symmetric pair of fixed points $(x, y, z) = (\pm\sqrt{b(r-1)}, \pm\sqrt{b(r-1)}, r-1)$.

Remark: Imaginary fixed points (sometimes called 'ghosts') can have a significant influence on the dynamics, particularly as they approach a bifurcation.

6.6 Periodic Orbits

Locating periodic orbits in a flow is far more difficult than finding the fixed points of a flow. However, the periodic orbits in a flow are a key ingredient in the description of the chaotic behavior of a dynamical system. In fact, the classification of low dimensional chaotic dynamical systems depends in a fundamental way on the unstable periodic orbits which are all but invisible in such systems. It is therefore useful to describe methods for finding periodic orbits and assessing their stability.

6.6.1 Locating Periodic Orbits in $R^{n-1} \times S^1$

The problem of finding periodic orbits is simplified to some extent if the phase space for the flow has the topology of a torus: $R^{n-1} \times S^1$. It is then often possible to construct a first return map $R^{n-1} \to R^{n-1}$ which describes how a Poincaré section R^{n-1} at $S^1(\theta)$ is mapped into itself as θ increases to $\theta + 2\pi$. If we represent this map by

$$\begin{aligned} x_1' &= f_1(x_1, x_2, \cdots, x_{n-1}) \\ x_2' &= f_2(x_1, x_2, \cdots, x_{n-1}) \\ &\vdots \\ x_{n-1}' &= f_{n-1}(x_1, x_2, \cdots, x_{n-1}) \end{aligned} \tag{6.50}$$

then the problem of finding the period one orbits becomes equivalent to the problem of finding the zeroes of the functions $x_i - f_i(x_1, x_2, \cdots, x_{n-1})$. If these functions are polynomials, then the *grobner* package described above can be used to find the zeroes of the difference map, or the period one orbits of the flow.

Higher period orbits are located using a standard procedure. The p^{th} iterate of the first return map is constructed, and its fixed points are located.

Example 1: The Henon map $R^2 \to R^2$ is invertible if $s \neq 0$:

$$\begin{bmatrix} x \\ y \end{bmatrix}' = \begin{bmatrix} a - (x^2 + y) \\ sx \end{bmatrix} \tag{6.51}$$

The Gröbner package identifies the two fixed points as

$$[sx - y, y^2 + (s^2 + s)y - as^2] \tag{6.52}$$

The second factor is to be solved for the two values of the y coordinate. Then the linear equation $sx - y = 0$ is used to solve for each corresponding x coordinate.

Example 2: The cusp map $R^2 \to R^2$ is not invertible:

$$\begin{bmatrix} x \\ y \end{bmatrix}' = \begin{bmatrix} a_1 - y \\ a_2 - (x^3 + xy) \end{bmatrix} \tag{6.53}$$

The Gröbner package identifies the three fixed points as

$$[-a_1 + x + y, y^3 + (-3a_1 + 1)y^2 + (-1 - a_1 + 3a_1^2)y + (a_2 - a_1^3)] \tag{6.54}$$

The second factor is to be solved for the three values of the y coordinate. Then the linear equation $x + y - a_1 = 0$ is used to solve for each corresponding x coordinate.

6.6.2 Bifurcations of Fixed Points

Bifurcation sets for maps are described in exactly the same way as bifurcation sets for flows. We illustrate with two examples.

Example 1: The y coordinates for the fixed points of the invertible ($s \neq 0$) Henon map (6.51) are obtained from (6.52)

$$y_\pm = -\frac{1}{2}(s^2 + s) \pm \sqrt{\left(\frac{1}{2}(s^2 + s)\right)^2 + as^2} \tag{6.55}$$

There are two real fixed points when $(s + 1)^2 + 4a > 0$. The bifurcation set is defined by $(s + 1)^2 + 4a = 0$.

Example 2: The bifurcation set for the noninvertible cusp map (6.53) is defined by the double degeneracy of the roots of the cubic equation which appears in (6.54). The condition for root degeneracy is imposed as follows:

$$\begin{array}{lccccccccc} \text{roots of cubic :} & y^3 & + & Ay^2 & + & By & + & C & = & 0 \\ \text{degeneracy condition :} & 3y^2 & + & 2Ay & + & B & & & = & 0 \end{array} \tag{6.56}$$

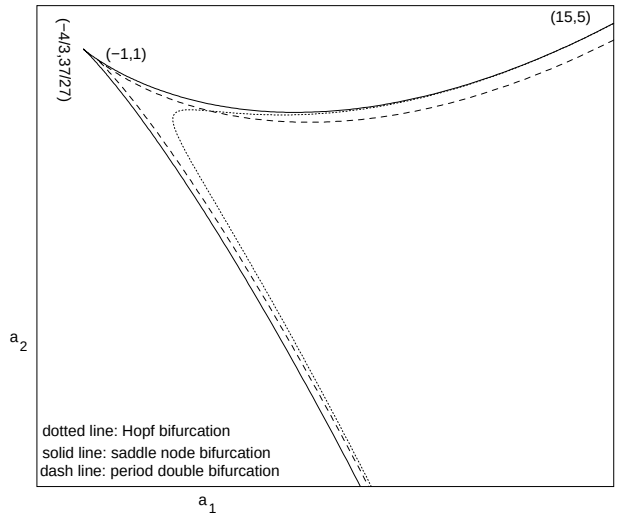

Figure 6.6: Two fold lines form the bifurcation set for the noninvertible cusp map (6.53). On crossing a fold line from inside the cusp-shaped region to outside, the interior and one of the two exterior real fixed points collide, become degenerate, and scatter off each other to become a complex conjugate pair.

These two equations provide a parametric representation for the bifurcation set $(a_1(y), a_2(y))$ in terms of a dummy variable y. The bifurcation set is shown in Fig. 6.6. It consists of two components ("fold lines"). In the cusp-shaped region there are three real fixed points with y coordinate values $y_1 < y_2 < y_3$. The interior fixed point becomes degenerate with one of the two outside fixed points when either of the fold lines is crossed. The dummy variable is the y coordinate of the doubly degenerate fixed point.

6.6.3 Stability of Fixed Points

The stability of periodic orbits is determined by linearizing the first return map in the neighborhood of fixed points. If x^* is a fixed point of a first return map, then

$$(x^* + \delta x)'_i = f_i(x^* + \delta x) = f_i(x^*) + \left.\frac{\partial f_i}{\partial x_j}\right|_{x^*} \delta x_j \tag{6.57}$$

In particular, the stability is determined from the eigenvalues of the Jacobian matrix

$$J = \left[\frac{\partial f_i(x^*)}{\partial x_j}\right] \tag{6.58}$$

The fixed point is stable if all eigenvalues $\lambda_i(c)$ are smaller than one in absolute value: $|\lambda_i(c)| < 1$. The fixed point of the map is unstable in k directions if k eigenvalues have magnitude larger than one. If one or more eigenvalues

have magnitude equal to one, then bifurcations can be expected as the control parameters are swept from $c - \delta c$ to $c + \delta c$.

Example: The Jacobian of the invertible Henon map (6.51) is

$$J = \begin{bmatrix} -2x & -1 \\ s & 0 \end{bmatrix} \tag{6.59}$$

The two eigenvalues of this matrix are $\lambda_\pm = -x \pm \sqrt{x^2 - s}$. The x coordinates of the fixed points are $x_\pm = -\frac{1}{2}(s+1) \pm \sqrt{(\frac{1}{2}(s+1))^2 + a}$. At the A_2 bifurcation to two real fixed points, one of the two is stable and the other is unstable in one direction.

6.7 Flows Near Nonsingular Points

In the neighborhood of a nonsingular point $\bar{x}$ it is possible to find a local diffeomorphism which brings the flow to a simple canonical form. The canonical form is

$$\begin{aligned} \dot{y}_1 &= 1 \\ \dot{y}_j &= 0 \qquad\qquad j = 2, 3, \cdots, n \end{aligned} \tag{6.60}$$

The transformation to this canonical form is shown in Fig. 6.7.

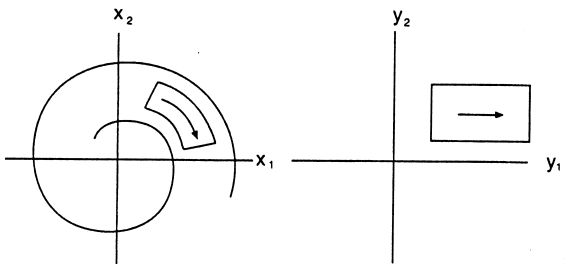

Figure 6.7: A smooth transformation reduces a dynamical system to the very simple local normal form (6.60) in the neighborhood of a nonsingular point.

The local normal form (6.60) tells us nothing about how the phase space is stretched and squeezed locally by the flow. To provide this information, at least locally, we present another version of this local normal form theorem that is much more useful for our purposes. If $\bar{x}$ is not a singular point, then there is an orthogonal (volume-preserving) transformation, centered at $\bar{x}$, to a new coordinate system in which the dynamical equations assume the following local canonical form in the neighborhood of $\bar{x}$:

$$\begin{aligned} \dot{y}_1 &= |F(x,c)| = \left(\sum_{k=1}^{n} F_k(\bar{x},c)^2 \right)^{1/2} \\ \dot{y}_j &= \lambda_j(\bar{x},c) \qquad j = 2, 3, \cdots, n \end{aligned} \tag{6.61}$$

The local eigenvalues $\lambda_j(\bar{x}, c)$ describe how the flow deforms phase space in the neighborhood of $\bar{x}$. This deformation is illustrated in Fig. 6.8. The constant associated with the y_1 direction shows how a small volume is displaced by the flow in a short time Δt. If $\lambda_2 > 0$ and $\lambda_3 < 0$, the flow stretches the initial volume in the y_2 direction and shrinks it in the y_3 direction. The exponents $\lambda_j(\bar{x}, c)$ are called *local* Lyapunov exponents.

Remark: One eigenvalue of a flow at a nonsingular point always vanishes, and the associated eigenvector is the flow direction.

remark to myself - do a nice, intuitive job to explain this point.

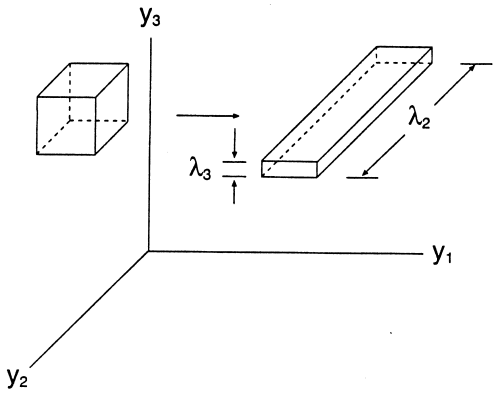

Figure 6.8: Orthogonal transformation reduces a dynamical system to the very simple local normal form (6.61) in the neighborhood of a nonsingular point. The local Lyapunov exponents describe how the edges of the cube of initial conditions expand or contract.

6.8 Volume Expansion/Contraction

Under the flow, a small region in phase space will change shape and size, as can be seen in Fig. 6.8. The time rate of change of the volume of the region is determined by the divergence theorem.

We assume that a small volume V in phase space is bounded by a surface $S = \partial V$ at time t, and ask how the volume changes during a short time dt. The volume will change because the flow deforms the surface. The change in the volume is equivalent to the flow through the surface. The volume change can be expressed as

$$V(t + dt) - V(t) = \oint_{\partial V} dx_i \wedge dS_i \tag{6.62}$$

Here dS_i is an element of surface area which is orthogonal to the displacement dx_i and $\wedge$ is the standard mathematical generalization to R^n of the vector cross

product in R^3. The time rate of change of volume is

$$\frac{dV}{dt} = \oint_{\partial V} \frac{dx_i}{dt} \wedge dS_i = \oint_{\partial V} F_i \wedge dS_i \tag{6.63}$$

The surface integral is related to a volume integral by

$$\frac{1}{V}\frac{dV}{dt} = \lim_{V \to 0} \frac{1}{V} \oint_{\partial V} F_i \wedge dS_i \stackrel{\text{def}}{=} \text{div}F = \nabla \cdot F \tag{6.64}$$

In a locally cartesian coordinate system, $\text{div}F = \sum_{i=1}^{n} \frac{\partial F_i}{\partial x_i}$. The divergence can also be expressed in terms of the local Lyapunov exponents:

$$\text{div}F = \sum_{j=1}^{n} \lambda_j(\bar{x}, c) \tag{6.65}$$

where $\lambda_1 = 0$ (flow direction) and λ_j $(j > 1)$ are the local Lyapunov exponents in the direction transverse to the flow direction. This is a direct consequence of the local normal form result (6.61).

6.9 Stretching and Squeezing

In this work we are principally interested in chaotic motion. Roughly speaking, this is motion which is recurrent but nonperiodic in a bounded region in phase space. Chaotic motion is defined by two properties:

(a) Sensitivity to initial conditions

(b) Recurrent nonperiodic behavior

Sensitivity to initial conditions means that two nearby points in phase space "repel" each other. That is, the distance between two initially nearby points increases exponentially in time, as least for sufficiently small time:

$$d(t) = d(0)e^{\lambda t} \tag{6.66}$$

Here $d(t)$ is the distance separating two points at time t, and $d(0)$ is the initial distance separating them at time $t = 0$, t is sufficiently small, $d(0)$ is sufficiently small, and the "Lyapunov exponent" λ is positive.

To put it graphically, two nearby initial conditions are "stretched apart."

If two nearby initial conditions diverged from each other exponentially in time for all times, they would wind up at opposite ends of their universe (phase space). If the motion in phase space is bounded, then the two points will eventually reach a maximum separation and then begin to approach each other again.

To put it graphically again, the two points are "squeezed together."

Chaotic motion is generated by the repetitive action of these two processes. Specifically, a strange attractor is built up by the repetition of the stretching

and squeezing processes. It is this repetitiveness which is responsible for the self-similar geometry of strange attractors. More to the point, if we understand how to choose some appropriate piece of phase space, and if we know the nature of the stretching and squeezing processes, then we have an algorithm for constructing strange attractors from the given input and the two processes acting together.

We illustrate these ideas in Fig. 6.9 for a process that develops a strange attractor in R^3. We begin with a set of initial conditions in the form of a cube. As time increases, the cube stretches in directions with positive local Lyapunov exponents and shrinks in directions with negative local Lyapunov exponents. Two typical nearby initial conditions (a) separate at a rate determined by the largest local Lyapunov exponent (b). Eventually these points reach a maximum separation (c), and thereafter are squeezed to closer proximity (d). If the initial neighborhood is chosen properly, then the image of the neighborhood may intersect the original neighborhood after a finite time (e),(a). This stretching and squeezing is then repeated, over and over again, to build up a strange attractor.

Remark: We make a distinction between "shrinking," which must occur in a dissipative system since some eigenvalues must be negative (*c.f.*, (b), $\sum_{i=1}^{n} \lambda_i < 0$), and "squeezing," which forces distant parts of phase space together.

Remark: When squeezing occurs, the two distant parts of phase space which are being squeezed together must be separated by a boundary layer. This boundary layer is indicated in (d). Boundary layers in dynamical systems are important but have not been extensively studied.

Remark: The intersection of the original neighborhood with its image under the flow creates the possibility of having fixed points in the first-, second-, $\cdots$, p^{th}-return maps. These fixed points identify period-one, -two, $\cdots$, -p orbits in the flow.

6.10 The Fundamental Idea

The stretching and squeezing processes, repeated over and over again in phase space, act to generate chaotic behavior and to build up strange attractors.

Many different stretching and squeezing processes exist. For example, the strange attractors which are generated by the Duffing, van der Pol, Lorenz, and Rössler systems are built up by four inequivalent stretching and squeezing processes. This means, in particular, that no diffeomorphism exists which maps any one of these sets of equations into any of the others. They are distinct and inequivalent at a fundamental (topological) level.

Embedded in each strange attractor is a large collection of periodic orbits. In three dimensions these orbits are rigidly organized with respect to each other. The organization is determined by the particular stretching and squeezing mechanism which acts to build up the strange attractor. Each different stretching and squeezing mechanism generates a different organization of periodic orbits in the host strange attractor.

Fundamental Idea: We will identify strange attractors, as well as the stretching and squeezing mechanisms which generate them, by identifying the

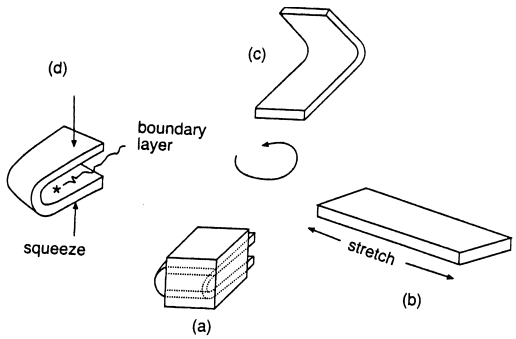

Figure 6.9: A cube of initial conditions (a) evolves under the flow. The cube moves in the direction of the flow. The sides stretch in the direction of the positive local Lyapunov exponents and shrink in the direction of the negative local Lyapunov exponents (b). Eventually two initial conditions reach a maximum separation (c) and begin to get squeezed back together (d). A boundary layer separates distant parts of phase space that are squeezed together. The image of the cube, under the flow, may intersect the original neighborhood (e),(a). Repetition of the stretching and squeezing processes builds up a layered structure which is self-similar. This geometric object is called a strange attractor. The stretching and squeezing mechanisms also create large numbers of periodic orbits which are organized among themselves in a unique way. This organization is the Achille's Heel for understanding strange attractors.

organization of the periodic orbits "in" the strange attractor. The organization of the orbits in turn is determined by a spectrum of names for the orbits (symbolic dynamics) together with a set of topological indices for each orbit and each pair of orbits. These indices, linking numbers and relative rotation rates, will be discussed in the following Chapter.

In short, periodic orbits provide the fingerprints for identifying strange attractors and the stretching and squeezing mechanisms which generate them.